



Paul Kindlhofer, BSc

# Fabrication of Thermoresponsive Hydrogel Double-Layers via Initiated Chemical Vapor Deposition

**Master's thesis**

to achieve the university degree of

Dipl.-Ing.

Master's degree programme: Technische Physik

submitted to

**Graz University of Technology**

Supervisor

Assoc.Prof. Dr. Anna Maria Coclite

Institute of Solid State Physics

Vienna, July 2020

---

## Affidavit

I declare that I have authored this thesis independently, that I have not used other than the declared sources/resources, and that I have explicitly indicated all material which has been quoted either literally or by content from the sources used. The text document uploaded to TUGRAZonline is identical to the present master's thesis.

---

Date

---

Signature

# Abstract

Thermoresponsive p(NVCL-co-DEGDVE) single-layers and, for the first time, also double-layers are fabricated via iCVD. By changing the crosslinker fraction incorporated in the thin films, their properties can be altered, resulting in films with responses at different temperatures. With a lower filament temperature and the introduction of nitrogen gas in the deposition process, even lower phase transitions can be obtained, although the degree of swelling decreases, as their transition temperature shifts towards lower values.

Three double-layers, with different structure and properties are fabricated, whereas only one of them exhibits a response at two separate temperature values.

# Zusammenfassung

Mittels iCVD werden thermoresponsive p(NVCL-co-DEGDVE) Einzelschichten, sowie, zum ersten Mal auch, Doppelschichten hergestellt. Durch Änderung des in den Dünnschichten enthaltenen Anteils an Vernetzern, können deren Eigenschaften in gewünschter Weise geändert werden. Dadurch ist es möglich Schichten, welche bei unterschiedlichen Temperaturen reagieren, herzustellen. Durch die Verwendung einer niedrigeren Filament Temperatur und dem Einsatz von Stickstoff während des Syntheseprozesses, können Phasenübergänge bei noch niedrigeren Temperaturen realisiert werden, wobei dadurch zeitgleich auch das Schwellvermögen der Schichten abnimmt. Drei Doppelschichten, mit unterschiedlichem Aufbau und Eigenschaften wurden hergestellt, nur eine weist Reaktionen bei zwei unterschiedlichen Temperaturwerten auf.

# Acknowledgments

First of all, I want to thank my supervisor Assoc.Prof. Anna Maria Coclite, who was there for me all the time I needed something. She helped me with her knowledge about the iCVD setup and with understanding the different polymerization processes taking place inside it, as well as with her optimistic nature.

Special thanks also goes to Fabian Muralter, who did pioneer work in the field of thermoresponsive hydrogel thin films. Even though he spent a semester in the US, he always was available for answering my questions and passing on his knowledge. Furthermore, Katrin Unger needs to be mentioned here, since her willingness to help and to find solutions to problems that arose during my work in the lab, was invaluable.

I also want to pay tribute to the work of Harald Kerschbaumer, who was often the most needed person in the institute, but still managed to repair, replace or build up devices, which were crucial for the progress of the thesis. The working group of Anna warmly welcomed me, and over the past year I learned to appreciate everyone of them. The same has to be said about the master students, with whom I shared the office.

Last but not least, I want to thank my family and my girlfriend, for always supporting me through all the years of study and helping me get up again, after experiencing setbacks. You are the best.

# List of Figures

1.1. Multi-layer, responsive in different temperature regimes and its corresponding swelling curve . . . . .	2
2.1. Phase diagram of a hydrogel with LCST . . . . .	4
2.2. Swelling curve . . . . .	5
2.3. Structural formular of NVCL & pNVCL . . . . .	8
2.4. Structural formular of Di(ethylene glycol) divinyl ether (DEGDVE) . . . . .	9
2.5. Structural formular of p(NVCL-co-DEGDVE) . . . . .	10
2.6. Working principle of a Spectroscopic Ellipsometry (SE) measurement . . . . .	15
2.7. Flow chart for ellipsometry data analysis . . . . .	17
3.1. Schematic of the iCVD reactor . . . . .	20
3.2. Model used for fitting ellipsometry data . . . . .	26
3.3. LCST evaluation . . . . .	29
3.4. Error estimation . . . . .	30
4.1. Degree of swelling as a function of DEGDVE needle valve opening . . . . .	33
4.2. Swelling curve and Lower Critical Solution Temperature (LCST) position of 3 differently crosslinked films . . . . .	34
4.3. LCST as a function of the crosslinker fraction represented by the swelling degree . . . . .	35

## List of Figures

---

4.4. Swelling curve of 2 differently crosslinked samples, fabricated at a filament temperature of 175 °C, compared with the highest crosslinked sample fabricated at a filament temperature of 200 °C. . . . .	38
4.5. Schematic of the 1st double-layer . . . . .	40
4.6. Swelling curve of 1st double-layer and both single-layers . . .	40
4.7. Swelling curve of 1st double-layer and theoretical, independent double-layer . . . . .	42
4.8. Schematic of the 2nd double-layer . . . . .	43
4.9. Swelling curve of 2nd double-layer and both single-layers . .	44
4.10. Swelling curve of 2nd double-layer and theoretical, independent double-layer . . . . .	46
4.11. Schematic of the 3rd double-layer . . . . .	47
4.12. Swelling curve of 3rd double-layer and both single-layers . .	48
4.13. Swelling curve of 3rd double-layer and theoretical independent double-layer . . . . .	49

# Contents

<b>1. Introduction</b>	<b>1</b>
<b>2. Basics</b>	<b>3</b>
2.1. Stimuli-responsive Hydrogels . . . . .	3
2.2. Thermoresponsive Hydrogels . . . . .	4
2.2.1. Lower Critical Solution Temperature . . . . .	6
2.2.2. N-Vinylcaprolactam . . . . .	7
2.2.3. Crosslinker . . . . .	9
2.3. Initiated Chemical Vapor Deposition . . . . .	11
2.4. Spectroscopic Ellipsometry . . . . .	14
<b>3. Experimental Setup</b>	<b>19</b>
3.1. iCVD Reactor . . . . .	19
3.1.1. Thin Film Fabrication . . . . .	21
3.2. Spectroscopic Ellipsometer . . . . .	26
3.2.1. Thin Film Characterization . . . . .	26
<b>4. Experiments</b>	<b>31</b>
4.1. Single-Layers . . . . .	31
4.1.1. Tune LCST by change of crosslinker fraction . . . . .	32
4.1.2. Tune LCST by changing the filament temperature & introducing nitrogen flow . . . . .	36

## Contents

---

4.2. Double-Layers . . . . .	39
4.2.1. First Double-Layer . . . . .	39
4.2.2. Second Double-Layer . . . . .	43
4.2.3. Third Double-Layer . . . . .	47
<b>5. Conclusion</b>	<b>51</b>
<b>A. Abbreviations</b>	<b>55</b>
<b>Bibliography</b>	<b>56</b>

# 1. Introduction

The ERC-project "Smart Core/shell nanorods arrays for artificial skin Smart Core" aims to create a temperature-, humidity- and pressure-sensing device, by fabricating stimuli-responsive nanorods, suitable for artificial skin applications. Those nanorods show a core-shell structure, where the core is a multi-stimuli-responsive polymer covered by a piezoelectric ZnO shell. A stimuli induces volumetric changes in the smart polymer, resulting in pressure on the piezoelectric material, which then can be read out as an voltage pulse.

The objective of this master thesis is to fabricate a thin film, responsive to humidity and different temperature regimes, that can be used as the core material of the nanorods. For this purpose, the co-polymer p(NVCL-co-DEGDVE) is chosen, because it undergoes a phase transition from a swollen to a collapsed state at a specific temperature value, the so called LCST, if immersed in water. Furthermore it has been shown that, besides its biocompatibility [1], p(NVCL-co-DEGDVE) also has an ultrafast response to humidity [2]. To realize a thin film, responsive in different temperature regimes, a multi-layer, consisting of single-layers with different LCSTs has to be fabricated. Its change of thickness or degree of swelling, while being exposed to temperature is called the swelling curve and has to fulfill certain criteria. The individual layers must have sharp phase transitions, which do not overlap, to gain a combined swelling curve, similar to a step function (see fig. 1.1). Also their degree of swelling has to be comparable and should

## 1. Introduction

---

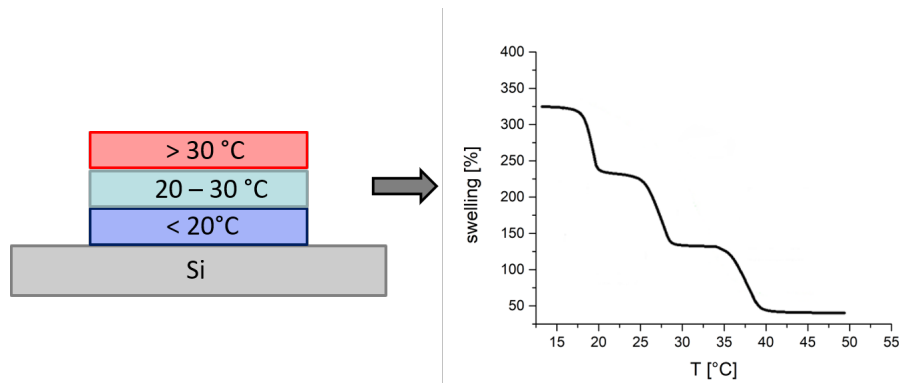


Figure 1.1.: left: Multi-layer, responsive in different temperature regimes, right: corresponding swelling curve

be at least around 200 %. Initiated Chemical Vapor Deposition (iCVD) is chosen for the thin film synthesis, since its many advantages of other deposition techniques, like conformal coating or the retention of functional groups of the used components.

The fabricated thin films are then analyzed via SE, regarding their change in thickness and degree of swelling as a function of the temperature.

The first part deals with the fundamentals of thermoresponsive hydrogels, their synthesis, and the characterization methods.

The experimental setup and methodology of thin film fabrication and characterization is described in the second part.

The third part consists of experiments on how to tune the properties of a thermoresponsive single-layer, as well as experiments on the behavior of the fabricated double-layers.

## 2. Basics

### 2.1. Stimuli-responsive Hydrogels

Hydrogels in general are three dimensional polymer networks, connected either via physical bonds (e.g. entanglement, hydrogen bonds, hydrophobic interactions) or chemical bonds. Due to the hydrophilic nature of the polymer structure, they are able to absorb large amounts of water without dissolving, leading to a volumetric change of multitudes compared to their dry size [3]. Together with their soft physical properties, which match those of living tissue, hydrogels are excellent biomaterials [4].

Compared to ordinary hydrogels, stimuli-responsive hydrogels are considered to have an even higher impact in various applications, since they have the ability of responding reversibly to physical and/or chemical stimuli in the environment, like temperature, pH, electromagnetic fields, radiation etc.[5]. Such properties make stimuli-responsive hydrogels a promising candidate in different fields, such as sensors [6] and actuators [7], controlled drug delivery [8] or tissue engineering [5].

A fast response, as well as a large response amplitude to a small stimuli is the main requirement for such a material. [9]

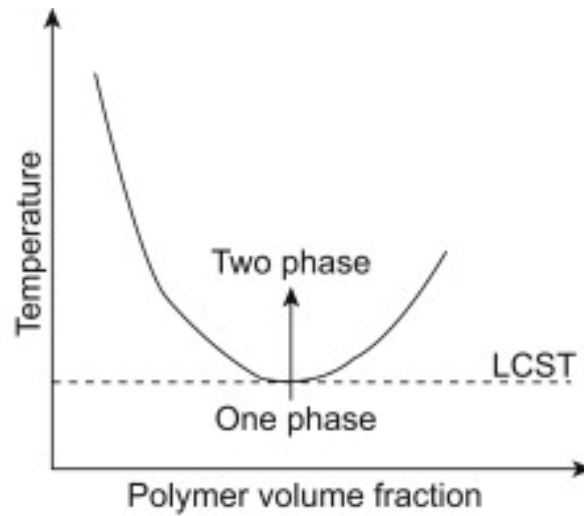


Figure 2.1.: Phase diagram of a hydrogel with LCST, reprinted from [10].

## 2.2. Thermoresponsive Hydrogels

In the case of thermoresponsive polymers, the stimulus that introduces changes in the polymer's structure is the environmental temperature. If the polymer is immersed in water or exposed to humidity, the change of temperature induces a phase transition at the so called LCST, where the hydrogel transitions from a hydrophilic (swollen) state at temperatures below the LCST, to a hydrophobic (collapsed) state, if the temperature value is raised above the LCST. This behavior is described by the phase diagram shown in figure 2.1.[5].

At temperatures below the LCST, the polymer-water phase is stable, until it reaches the LCST and a phase transition takes place, where the single phase gets unstable and separates into two phases, namely, the collapsed polymer mesh and the repelled water. This phase transition induces changes, as mentioned above, in the polymer's properties. One of those affected

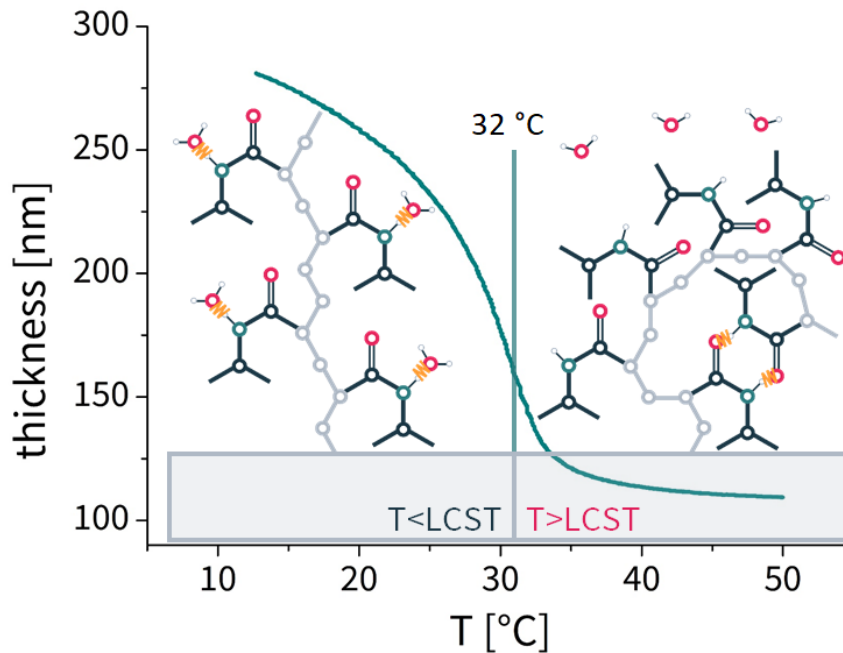


Figure 2.2.: Change of film thickness, while heating up a thermoresponsive hydrogel, courtesy of Fabian Muralter.

properties is the volumetric change, which in the case of hydrogel thin films, is the change in film thickness. The temperature-dependent progression of the film thickness, as well as the change of the polymer structure can be seen in figure 2.2.

At temperatures below the LCST, the hydrogel is in the swollen state, where it reaches its maximum thickness value. This comes from the fact, that the polymer backbone (illustrated in grey) assumes a coil structure, therefore the hydrophilic parts (illustrated in light blue) can form hydrogen bonds with water. At temperatures above the LCST, a switch from hydrophilicity to hydrophobicity occurs and the hydrogel transitions into the collapsed state. The polymer network repels the water molecules, because it favors intramolecular bonds in this temperature regime. That causes the backbone

to bend and therefore the film thickness is reduced.[11].

Since this swelling-deswelling behavior is reversible, thermoresponsive hydrogels are promising candidates for humidity- and temperature-sensing applications.[7]

### 2.2.1. Lower Critical Solution Temperature

The LCST is defined as the inflection point of the swelling curve and divides the status of the polymer into swollen and collapsed state. It is strongly affected by the molecular weight of the polymerized material [12]. By changing the molecular weight, which is accomplished by the variation of the polymer chain length, the repelling-mechanism of water molecules and therefore the deswelling behavior is altered.

With longer molecule chains, the ability of bending the backbone is increased and intramolecular bonds can be formed more easily, leading to LCSTs at lower temperature values and vice versa.

Another parameter, that can change the LCST position, is the copolymerization with a second species. By using either a more hydrophilic or hydrophobic monomer, added to the monomer, which is used to form the thermoresponsive polymer, the LCST shifts either to higher or lower temperature values. A thermoresponsive copolymer, which is more hydrophilic than the thermoresponsive homopolymer, favors hydrogen bonding over a longer temperature range (higher LCST), while a more hydrophobic copolymer repels the water molecules out of the polymer network at even lower temperatures, resulting in a lower LCST.[13].

### 2.2.2. N-Vinylcaprolactam

poly(N-Vinylcaprolactam) (pNVCL) is the second most prominent thermoresponsive polymer, just behind poly(N-isopropylacrylamide) (pNIPAAm). What makes pNVCL a good candidate for incorporating it in a humidity and temperature sensing device, is its LCST position between environmental and body temperature [14], its non-toxic nature, as well as its biocompatibility, which has not been proven for pNIPAAm at this point [1]. Their swelling behavior in water/humidity is comparable, the LCST is also in the same range of 31 - 34 °C in aqueous medium, with reversible phase transitions from swollen to collapsed state in water [14]. The difficult polymerization kinetics of pNVCL, compared to nNIPAAm, is the reason why it lags behind in popularity, although it already has applications in fields of cosmetics, as an anticlogging agent in pipelines and biomedical science [1].

It has been shown, that an increase in polymer chain length, shifts the LCST to lower temperatures, due to its classical Flory-Huggins miscibility behavior, stemming from its specific chemical structure [12]. By varying the polymer chain length, LCSTs in the range of 16 - 40 °C can be achieved [15].

The structural formula of both, NVCL monomer and pNVCL are shown in figure 2.3.

The NVCL monomer unit consists of a caprolactam ring, with an oxygen atom attached to it via a double bond and a vinyl-group attached to the nitrogen atom. The nitrogen atom is responsible for the hydrophilic behavior at temperatures below the LCST, where it favors hydrogen bonding. At temperatures above the LCST, the hydrophobic behavior stems from the fact, that the polymer can lower its internal energy by going into intramolecular bonding, particularly bonding of the nitrogen atom and the oxygen atom

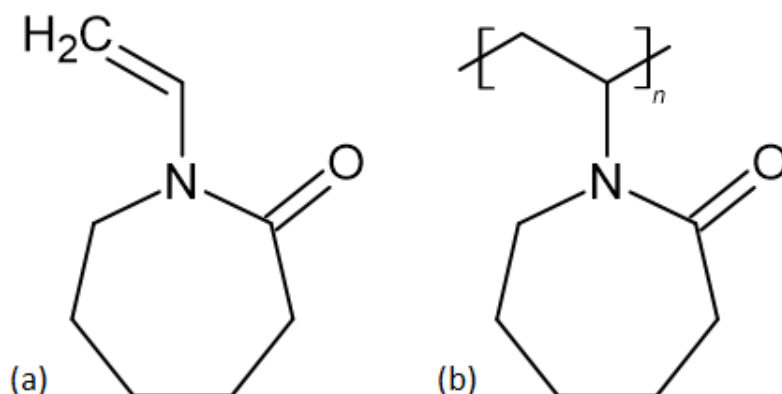


Figure 2.3.: (a) NVCL monomer unit, (b) pNVCL

and therefore, repelling the water molecules out of the polymeric structure [16].

If free radical initiators are used in the polymerization process, the vinyl-group is essential, which is activated by radical species from organic peroxides and starts the growth of the polymer backbone [17].

The outcome of the polymerization process with only using N-Vinylcaprolactam (NVCL) monomers is the pNVCL homopolymer, given in figure 2.3 (b), where the backbone is represented by the repeat unit.

Unfortunately a pNVCL homopolymer thin film dissolves from its substrate, if immersed in water. This can be attributed to the individual polymer chains, which are only connected via physical crosslinking. Because the polymer chains unfold in the swollen state, the intramolecular connection is entirely gone. As well, hydrolysis is taking place, where the water reacts with the polymer, fragmenting it in smaller pieces which then are soluble. To overcome this problem, a crosslinker has to be added in the polymerization process, to form thermoresponsive co-polymer with enhanced mechanical

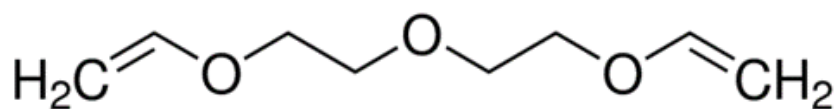


Figure 2.4.: Crosslinking agent DEGDVE, reprinted from [18]

stability and reduced solubility.

### 2.2.3. Crosslinker

The function of a crosslinker is to connect polymer chains of a homopolymer, resulting in a co-polymer with enhanced mechanical stability. DEGDVE is used as crosslinking monomer (structural formula in figure 2.4)

As visible in figure 2.4, the monomer unit has vinyl-groups on both ends, which will be activated by free radical initiators and therefore participates in the polymerization process, connecting the pNVCL polymer chains.

The outcome of a polymerization process, using both NVCL and DEGDVE monomers is the stable thermoresponsive polymer p(NVCL-co-DEGDVE), shown in figure 2.5

Besides the fact, that DEGDVE stabilizes the thermoresponsive thin film, it also has an effect on two other properties.

On the one hand, as mentioned above, the LCST of the fabricated co-polymer will differ from the LCST of the homopolymer, if the used crosslinker has a different hydrophobic/hydrophilic nature than the homopolymer. DEGDVE in particular, is more hydrophobic than pNVCL, which results in lower LCSTs with increasing crosslinker fraction [19]. This effect can be used for tailoring of the thin film's LCST.

On the other hand, a different crosslinker fraction leads to a change in the polymer's maximum degree of swelling, if the thin film is immersed in

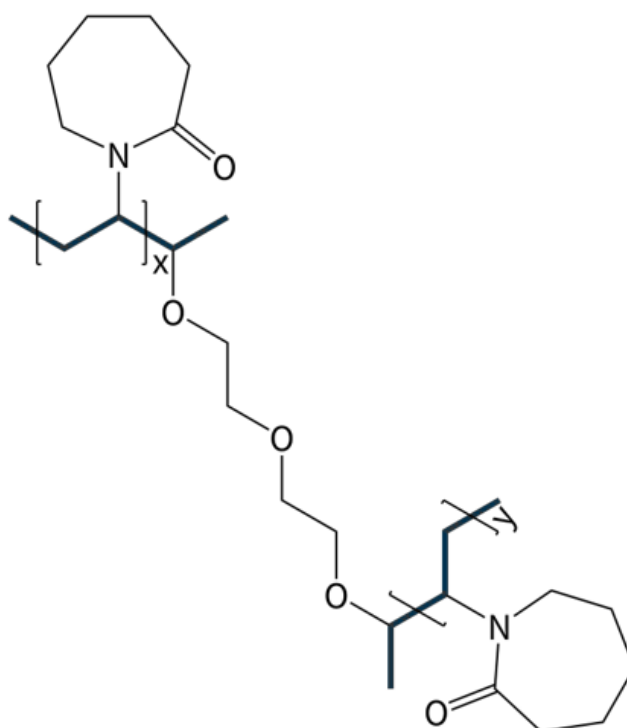


Figure 2.5.: Thermoresponsive co-polymer p(NVCL-co-DEGDVE), courtesy of Fabian Murrer.

water. The structure of a crosslinked hydrogel can be described as a polymer mesh. By increasing the amount of crosslinker in the hydrogel, the mesh size decreases and therefore lowers the amount of water, that can be taken up by the polymer mesh.[20].

### 2.3. Initiated Chemical Vapor Deposition

iCVD is a solvent-free polymerization technique, which allows the conformal coating of almost any surface. Furthermore the functional groups of the used monomers are retained, because it operates at relatively low temperatures, compared to other vapor deposition methods.[21].

The concept of iCVD relies on the introduction of initiator and monomer into a vacuum chamber, kept at a pressure typically between  $10^{-1}$  and 1 Torr, where the initiator molecules get thermally decomposed and radicalized at heated filament wires, that have temperatures between 200 and 400 °C. Those activated radicals then start polymerization of the monomer on a cooled surface (less than 50 °C) to promote adsorption [22].

The detailed reactions happening in the iCVD process are shown below.

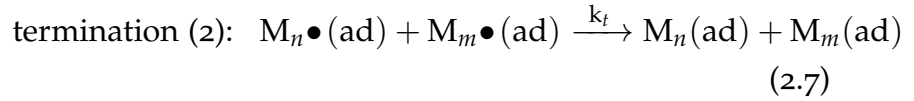
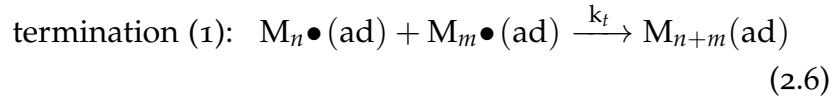
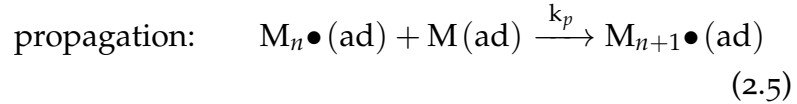
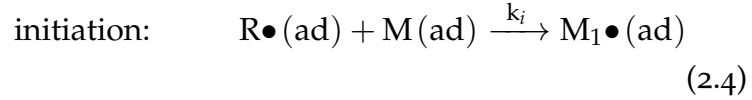
gas phase reaction:



gas to surface processes:



surface reactions:



As described in equ. (2.1) the initiators, introduced to the vacuum chamber, are thermally decomposed, in the gas phase, at the heated filament wires into 2 primary radicals (radicalized reactants are labelled with a dot in the equations). They are highly reactive, due to the unpaired electron, which is the result of thermally breaking of, for instance, the oxygen bond of an initiator molecule. By external cooling of the substrate-surface, a thermal gradient towards it is created, which forces the primary radicals and the monomers to adsorb mainly on this area. This process is described by equ. (2.2.) & (2.3). Polymerization starts, because the adsorbed primary radicals attack the  $\text{CH}_2$ -bonds of the monomers and thereby radicalize them (equ. (2.4)). After this initiation process, the resulting polymer radicals can propagate the polymerization, by reacting with other monomers, leading to growth of the polymer chains, which can be seen in equ. (2.5). Termination of the polymerization is achieved, either by coupling (equ. (2.6)) or by

disproportionation (equ. (2.7)). In addition, the growth of the polymers can be terminated, if a polymer radical reacts with a primary radical, shown in equ. (2.8). Equ. (2.9) describes the possibility, that primary radicals can also recombine.[22].

All the processes mentioned above, have a certain probability to take place, which is described by the different reaction rate constants  $k_n$ .

Another crucial parameter in iCVD is the saturation ratio:

$$S = \frac{p_M}{p_{sat}} \quad (2.10)$$

where  $p_M$  is the partial pressure of the monomer and  $p_{sat}$  is the monomer's saturation pressure at a given temperature. On the one hand, the absorbed monomer concentration on a substrate of each used species can be tuned, by adjusting their saturation ration. On the other hand, by increasing the ratio of partial pressure and saturation pressure, the deposition rate also increases linearly. This linear dependency applies to the range, where  $\frac{p_M}{p_{sat}} \leq 1$ , because at values greater than 1 the system is in saturation and condensation becomes dominant .[17]

The deposition rate can further be changed by varying the temperature gradient in the reaction chamber, which depends on the substrate temperature and the filament temperature. The lower the substrate temperature, the higher is the adsorption rate of the monomers and initiator radicals and therefore the deposition rate increases. Changing the filament temperature, besides changing the temperature gradient, mainly alters the initiator decomposition rate, which leads to lower initiation rates (lower deposition rate), as well as termination rates (longer molecular chains).

## 2.4. Spectroscopic Ellipsometry

SE is an indirect method for measuring several quantities of thin films, like film thickness, the refractive index, the extinction coefficient, surface roughness etc. It is a non invasive technique, that is suitable for in-situ measurements [23]. However a model that describes the thin film's properties has to be generated and fitted to the experimental data, to get information about the thin film properties, because an exact equation can not be calculated direct from the measurement. With regression analysis all the experimental data, which is often over-determined, can be included for determining the solution [24].

Polarized light can be expressed as a superposition of two orthogonal light beams, namely the p-plane (parallel to the plane of incidence) and the s-plane (perpendicular ('senkrecht') to the plane of incidence). It can be classified into three different categories, depending on the phase shift and the amplitude of p- and s-plane.

1. linearly polarized light: equal amplitude and in phase
2. circular polarized light: equal amplitude, but out of phase by  $90^\circ$
3. elliptically polarized light: arbitrary amplitude and phase

SE utilizes the fact, that the electric field components of the p- and s-plane undergo different changes when travelling through materials.

In figure 2.6 the working principle of an SE measurement is illustrated.

The incident beam is linearly polarized and hits the sample at a certain angle. Due to interactions of the the light with the sample material, both components of the reflected light change in phase and amplitude, resulting in an elliptical polarization.

## 2. Basics

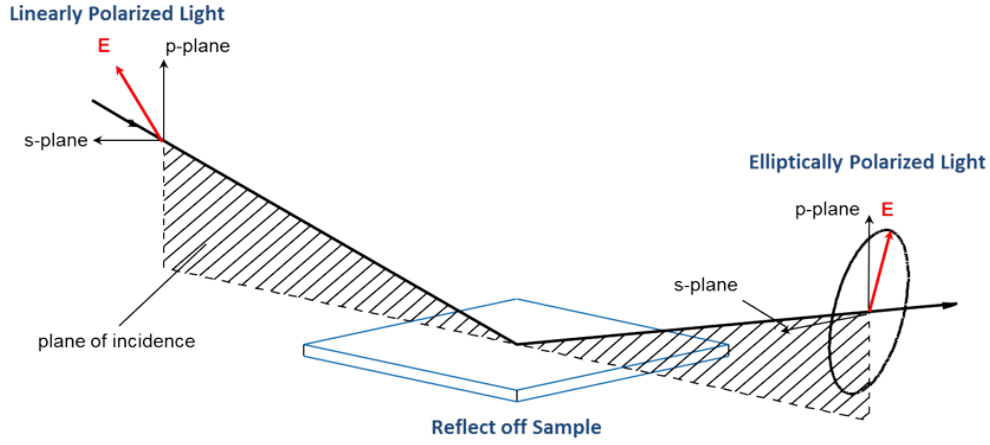


Figure 2.6.: Working principle of a SE measurement, reprinted by [25].

The outcome of such a measurement is the polarization change of the incident and outgoing/reflected beam  $\rho$ :

$$\rho = \tan(\psi)e^{i\Delta} = \frac{E_p^{out}/E_p^{in}}{E_s^{out}/E_s^{in}} = \frac{\tilde{r}_p}{\tilde{r}_s} \quad (2.11)$$

where  $\tan(\psi)$  is the ratio of the reflected amplitudes,  $\Delta$  is the phase shift of both electric field components,  $E^{out}$  &  $E^{in}$  are the amplitudes of the outgoing & incident electric field, and  $\tilde{r}$  stands for the Fresnel coefficient of reflection [26].

The Fresnel coefficients of reflection are connected to the index of refraction of the thin film via following relation, given by the Fresnel equation for non magnetic materials:

$$\tilde{r}_p = \frac{N_2 \cos(\theta_1) - N_1 \cos(\theta_2)}{N_2 \cos(\theta_1) + N_1 \cos(\theta_2)} \quad (2.12)$$

$$\tilde{r}_s = \frac{N_1 \cos(\theta_1) - N_2 \cos(\theta_2)}{N_1 \cos(\theta_1) + N_2 \cos(\theta_2)} \quad (2.13)$$

where  $N_1$  is the index of refraction of the surrounding environment,  $N_2$  is the thin film's index of refraction,  $\theta_1$  is the angle of the incoming and reflected light and  $\theta_2$  is the angle of the refracted beam in the film.

Information on the thickness  $d$  can be obtained by looking at the phase change from top to bottom of the film  $\beta$ :

$$\beta = 2 \pi \frac{d}{\lambda} N_2 \cos(\theta_2) \quad (2.14)$$

with  $\lambda$  being the wavelength of the used light [26].

As already mentioned, a model, that roughly defines the thin film's properties has to be generated, to fit the experimental data. For transparent and dielectric thin films, the Cauchy-model has proven to give reliable results. Its refractive index is related to the wavelength by the following dispersion relation:

$$n(\lambda) = A + \frac{B}{\lambda^2} + \frac{C}{\lambda^4} + \dots \quad (2.15)$$

$A$ ,  $B$  and  $C$  are the fitting parameters.  $A$  represents the refractive index value at high wavelengths, since in this range the refractive index gets almost constant for transparent materials. The change of optical properties in the shorter wavelength regime is taken into account by the following terms, where the use of fitting parameters  $B$  and  $C$  lead to satisfying solutions in a specific spectral range. This regression analysis is illustrated in figure 2.7

Subsequently, the ellipsometer-software adjusts the fitting parameters to find the best match between model and experimental data. The goodness of

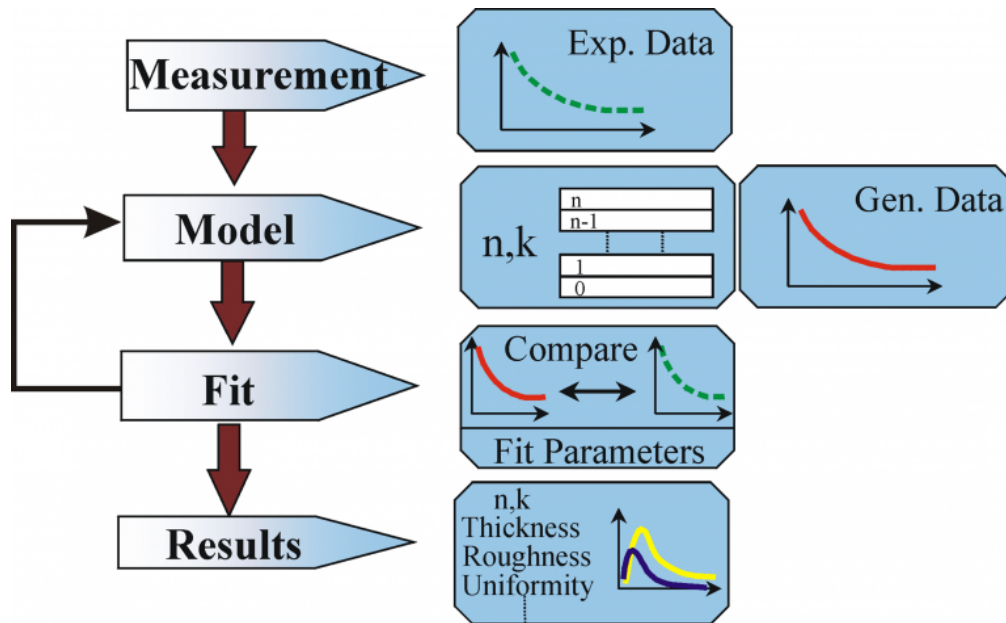


Figure 2.7.: Flow chart for ellipsometry data analysis, reprinted by [27]

the data generated by the model and the experiment fit is quantified by the Mean Squared Error (MSE). A smaller MSE implies a better fit.

Before starting to fit the model, an initiate guess for the fit parameters has to be done, to avoid the possibility of getting stuck in a local minima of the MSE function. By slightly adjusting the model and fit parameters after the first comparison, the match can be improved. This process can be stopped, if the result is satisfying.

Although, with SE a variety of thin film properties can be examined, just fitting a few parameters at the start is beneficial to find the lowest MSE and after that, other parameters of interest can be added.[24].

If the change of thickness, while heating up a thin film surrounded by water, should be measured, the model has to be expanded by a factor that considers on the one hand, the additional interfaces, namely the air-water- and the water-sample-interface, and on the other hand, the change of optical

## 2. Basics

---

properties of water at different temperatures.

## 3. Experimental Setup

### 3.1. iCVD Reactor

The thin film fabrication was performed in a custom-build iCVD reactor. In figure 3.1 a schematic of the iCVD setup is illustrated.

It consists of a cylindrical shaped reaction chamber with a removable quartz glass on top, to enable in-situ film thickness monitoring. This is achieved on the one hand by eye-observation, because the optical appearance of a growing transparent thin film changes due to interference with ambient light. On the other hand the film's thickness is monitored via laser interferometry, by using a laser (Thorlabs, HNLSoo8L-EC) with a wavelength fitted to the Fresnel equation for refractive indices of polymeric thin films ( $n \approx 1.5$ ). The change in power is measured by a detector, in our case a slope from the first power maximum to the next maximum corresponds to a thickness growth of 200 nm.

Inside the reaction chamber, an array of heatable filaments is installed, to radicalize the initiator agents. The temperature of the filaments can be set by a power supply and is monitored via a thermocouple, as well as the temperature of the substrate, which is regulated by a water cooling system (Thermo Scientific, Accel 500 LC).

### 3. Experimental Setup

---

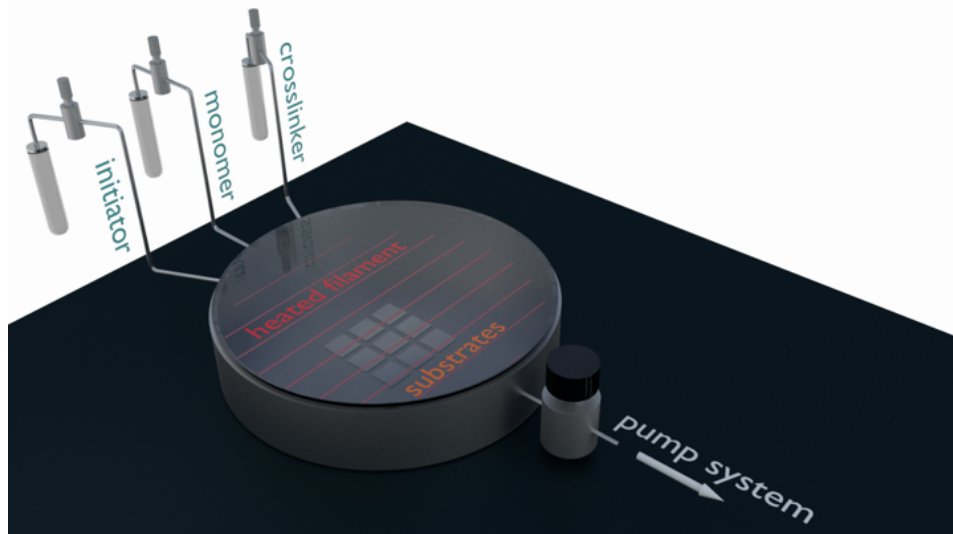


Figure 3.1.: Schematic of the iCVD reactor, courtesy of Fabian Muralter.

For introducing monomer-, crosslinker- and initiator-molecules into to reaction chamber, there are 4 separate lines available. In between the jars, where all the reactants are stored, and the reactor, there is one needle valve (Swagelok) attached to each line to control the vapor flow and one quarter-turn plug valve (Swagelok) for just opening and closing the connection completely. Furthermore, the lines are heated up to 90 °C, to avoid condensation.

Since the saturation pressure for some of the used reactants has to be enhanced to achieve suitable flowrates for the polymerization process, also external heating of the jars is provided.

In addition, there is a line for the introduction of Nitrogen existing.

The working pressure inside the reaction chamber is controlled by a throttle valve (MKS, 253B Exhaust Throttle Valve), which is installed prior to the pump system. The position of the valve is set by a pressure control unit (MKS, Pressure Controller 600 Series), where several preset programs can

be defined.

A pressure sensor is responsible for measuring the pressure. Together with a custom-made program, leakrate- and flowrate-estimation can be carried out. For both of them, the base pressure (lowest reachable pressure) has to be roughly reached, then in case of the leakrate-estimation, the throttle valve closes completely and the pressure rise over a predefined timescale is measured. The outcome gives information how free of leakage the system is.

For the flowrate-estimation, one monomer-line after each other has to be opened and again the change in pressure over time is measured. After the estimation, the leakrate is subtracted from the flowrate value, to display the correct flowrate value:

$$flowrate_{correct} = flowrate_{measured} - leakrate \quad (3.1)$$

A rotary vane pump (Pfeiffer Vacuum, Duo 65) is used to reach the medium vacuum regime, with a zeolite filter in front of it, to prevent toxic chemicals from getting into the pump.

Furthermore a quarter-turn plug valve is attached to the reactor, which is necessary for venting the vacuum system.

#### 3.1.1. Thin Film Fabrication

All fabricated thin films were deposited on single side polished Silicon wafers, with an native oxide layer of roughly 1.7 nm. For further investigations in the Heated Liquid Cell, they have to be cut in in pieces, with dimensions of 2 x 5 cm , to seal the cell from underneath.

### 3. Experimental Setup

---

After venting the iCVD reactor, which is achieved by closing the throttle valve and opening the quarter-turn plug valve, attached to the reaction chamber, the samples can be loaded. Due to the fact that the vapor pressure of NVCL is quite low, compared to most monomers used in iCVD processes, the deposition rate and film growth across the reactor is not uniform. Therefore the samples are placed in the same location throughout every deposition, to achieve comparable and reproducible results.

Closest to the outlet of the NVCL-line the film growth has a maximum, while it decreases at locations further away from the outlet. This problem can be overcome with the introduction of an inert gas such as nitrogen. The downside of this workaround is a drastic decrease in deposition rate, stemming from lower  $\frac{p_M}{p_{sat}}$  values of the participating reactants.

After the samples are placed in the iCVD reactor, the quarter-turn plug valve gets closed and the throttle valve gets completely opened, to get back to vacuum conditions needed for the polymerization process in the reaction chamber.

The next step is to fill reactant jars. In the beginning of the experiments, all three participants of the polymerization, namely NVCL, DEGDVE and Tert-Butyl peroxide (TBPO) were used until their jar was empty. This resulted in thermoresponsive thin films, with little swelling behavior and therefore broad LCSTs. Such a film's swelling curve can be seen in figure

By optical observation of the reactants, after one deposition, it was visible, that both remaining NVCL and DEGDVE in the jars have changed during the polymerization process.

In the case of NVCL on the one hand a change in color, from almost colorless to a slight yellow, can be seen, on the other hand, a phase change occurs. The pNVCL homopolymer has a melting point of 37 °C [28], to increase its vapor pressure it is heated up to 85 °C, but it is not solidifying

### 3. Experimental Setup

---

after a deposition, although it is cooling down to room temperature again. The used crosslinker DEGDVE also undergoes obvious structural changes, namely getting more and more viscous after each deposition.

Those changes in morphology indicate, that heating up those two monomers, as well as participating in the polymerization process seem to alter their reaction mechanisms.

To overcome this problem, the NVCL jar is cleaned and refilled after every deposition and the DEGDVE jar is cleaned and refilled after every second deposition. With this workflow it is possible to fabricate thermoresponsive thin films with a high degree of swelling and a sharp phase transition. The volatile initiator TBPO was not affected by successive depositions and could be used until its jar was empty.

After NVCL and DEGDVE are heated up to their desired temperature, to increase their vapor pressure, leakrate- and flowrate-estimation can be performed.

Flowrate values less than 0.09 standard cubic centimeters per minute (sccm) are accepted, higher values indicate residual particles from venting still being present in the reaction chamber and therefore the pump system needs to do further work. If a leakrate value below the mentioned value above is reached, the flowrate-estimation is following.

For this procedure, each monomer line is opened individually and the flowrate is measured at least three times, to confirm a stable value.

First the NVCL and the TBPO is estimated. For the NVCL flowrate, the needle valve opening is always in the maximum opening position, due to its low vapor pressure and varied between 0.1 - 0.3 sccm. This fluctuation will be discussed later.

The flowrate of TBPO is kept at 1 sccm throughout all the experiments.

With those flowrates and the vapor pressure of each reactant, at the set

### 3. Experimental Setup

---

temperature, the fraction of crosslinker present in the resulting thin film can be adjusted by following formula:

$$\text{crosslinker fraction [\%]} = \frac{(p_M/p_{sat})_{DEGDVE}}{(p_M/p_{sat})_{NVCL} + (p_M/p_{sat})_{DEGDVE}} \quad (3.2)$$

Unfortunately, the formula above is not leading to reliable results, meaning that a thin film with a calculated low crosslinker fraction did not show high swelling and high LCST and vice versa.

As mentioned above the low volatility of NVCL results in fluctuating flowrates, which can be attributed to the fact, that the pressure sensor measuring the pressure change during the flowrate-estimation is not close enough to the outlet of the NVCL line and therefore sometimes more of the monomer reaches the sensor, sometimes less. An attempt to overcome this problem is by introducing a preset nitrogen flow, adjusted via a flow controller, during the NVCL flowrate-estimation, to grant uniform monomer distribution in the reactor, but also this method is not leading to satisfactorily results.

To conquer this issue, the following methodology is applied. Before every deposition, a specific amount of NVCL is filled in the jar, which fulfills two criteria. First, the filling level, if liquefied, has to be at least above the round ending of the jar, to maximize the evaporation surface, second the amount that gets poured away should be minimized.

A mass of 1 g is found to satisfy both criteria for a 50 nm thin film and therefore is used in all the experiments. With this a reproducible flowrate can be expected, if the needle valve opening is kept in the same position (in this case: maximum opening).

### 3. Experimental Setup

---

Since the exact flowrate can not be measured, also the formula above can not be applied to estimate the crosslinker fraction that will be present in the fabricated thin film. Therefore the opening of the needle valve on the DEGDVE line, is taken as an indicator of the crosslinker fraction.

If all the jars are filled and their needle valves opened to a desired position, but still with closed quarter-turn plug valves, the substrate cooling can be started. Then the working pressure is set by the pressure control unit and all the quarter-turn plug valves are getting opened. If the required working pressure is reached, the filament heating is turned on by the power supply. At this point, the polymerization process starts.

The growth of the thin film is monitored in-situ via laser interferometry. If the wanted thickness is reached, the following steps have to be executed.

First, the lines of NVCL and crosslinker are getting closed, therefore only initiator radicals are present in the reaction chamber. As stated in section 2.3, only primary radical termination and primary radical recombination events can happen then, which stops the polymer chain growth. After 3 minutes, also the initiator line gets closed. Before completely opening the throttle valve, to pump out all the residual particles in the reactor, the power supply of the filament is switched off to avoid radicals entering and potentially damaging the pump system. If the filament temperature is below 100 °C the thermal energy is too low for radicalization and the evacuation can be started. Furthermore, the power supply of the jar-heating and the substrate cooling is switched off.

If the pressure inside the reaction chamber is at a value close to its base pressure, the system is vented and the fabricated thin film samples can be taken out.

### 3. Experimental Setup

---

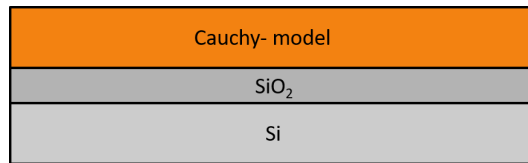


Figure 3.2.: Model used for fitting ellipsometry data.

## 3.2. Spectroscopic Ellipsometer

A J.A.Woollam ESM-300 Spectroscopic Ellipsometer was used to determine the optical properties of the fabricated p(NVCL-co-DEGDVE) thin films.

The measurements in deionized water are carried out in a J.A. Woollam Heated Liquid Cell. Since the cell is only able to heat up, the pre-cooling step is done in our lab fridge.

### 3.2.1. Thin Film Characterization

The sample properties, like thickness and refractive index, are then evaluated on the ellipsometer.

In figure 3.2, the model used for p(NVCL-co-DEGDVE) thin films deposited on a silicon wafer with an 1.7 nm native oxide layer is shown.

The model describing the silicon wafer with an native oxide layer is taken from the ellipsometer-software (CompleteEASE) The Cauchy-model is used for the transparent and dielectric p(NVCL-co-DEGDVE) hydrogel layer.

After the first thickness estimation, it is crucial to rinse the fabricated thermoresponsive thin films for 10 seconds with deionized water, because they are deposited in the collapsed state and there will be some rearrangements in the polymeric structure, as well as removal of loosely attached polymer

### 3. Experimental Setup

---

chains, while swelling. Following the rinsing process, the samples again are measured on the ellipsometer, where a loss of thickness in the range of 5 - 30 % can be seen. The obtained thickness value is taken as the thickness in dry state.

For the generation of the swelling curve, the thin film has to be put in the Heated Liquid Cell, where it is possible to immerse the sample completely in water and heat it up to 50 °C. The cooling process of the cell is done externally, in our lab's fridge.

The SE-library provides a feature, which takes the surrounding water and its change of optical properties, depending on the cell's temperature, into account.

The swelling curve is desired to always be measured from 10 - 50 °C, a temperature range, in which all possible LCST values should be contained. The temperature ramp is set to 0.5 °C/min, to ensure that the temperature in the cell can keep up with the temperature setpoint, as well as to minimize the time required for the measurement.

Since the lab, where the experiments are performed, is not air-conditioned, problems occurred on days with high humidity and temperatures above 20 °C. First, due to high temperatures, the pre-cooled Heated Liquid Cell already warms up above 10 °C in the time from taking the cell out of the fridge to having mounted the cell on the ellipsometer. With this, the temperature ramp is started at the lowest possible temperature possible (typically between 11 - 14 °C). Second, due to high humidity, condensation on the cell's windows occurs, which lowers the signal intensity reaching the detector to a value, where no information on the sample's properties can be made. This effect stems from the altered interactions at the interfaces. The condensation usually stops after the cell has reached temperatures above

### 3. Experimental Setup

---

15 °C, below that value the condensed water at the windows is removed continuously with cleaning paper.

In the first two heating cycles, changes in the thin film properties can be observed, like slight shifts of the LCST and the refractive index. These changes can be explained by the fact, that the initial heating cycles can be seen as a more intense rinsing process. First of all, during the external cooling, the thermoresponsive thin films swell to their greatest possible value, which causes polymer chains, that are not part of the hydrogel network, but are incorporated in it, to be pushed out of it. Furthermore, rearrangements in the polymeric structure will happen, activated by thermal energy available during the heating cycle.

For the LCST evaluation and the temperature dependent swelling behavior of the samples, the third heating cycle is taken [15].

For further investigations the data of the CompleteEASE software is transferred into Origin. Prior to the determining the LCST and the degree of swelling, the swelling curve is smoothed via a Savitzky–Golay filter. It is widely used in signal processing and has the advantage of not losing crucial signal information, while removing as much as possible noise. This is obtained by applying the least squares method on the convolution of chosen uniform data point sets, also called points of window [29]. By increasing the number of used points of window, the degree of smoothing as well increases.

As a measure of the swelling degree, the film thickness at 10 °C is taken and compared with their dry state thickness. For swelling curves not starting at 10 °C, due to reasons mentioned above, their thickness is estimated by their thickness change trend for measured values closest to the starting point of the temperature ramp.

Since the LCST is defined as the inflection point of the swelling curve, the

### 3. Experimental Setup

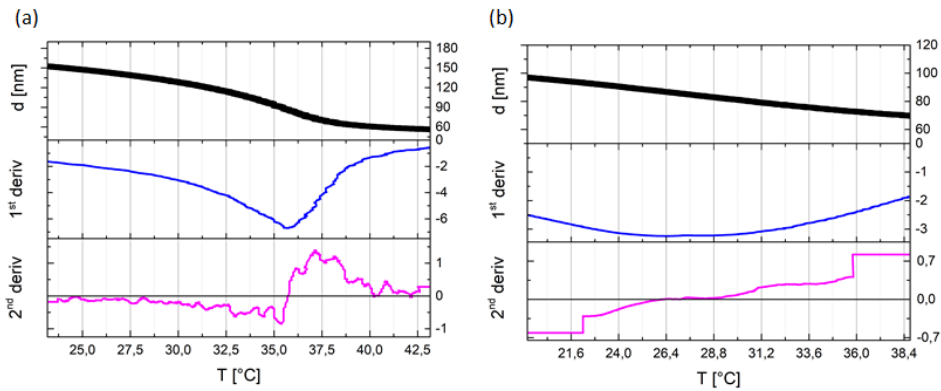


Figure 3.3.: (a) Sharp phase transition, (b) broad phase transition

value at the zero point of its second derivative is taken. For this purpose, the number of points of window used in the Savitzky–Golay filter is increased until only one point in the second derivative crosses the horizontal zero line. Two examples are given figure 3.3.

In figure 3.3(a) a sample with a sharp phase transition is illustrated. In this case the LCST position is distinct, compared to 3.3(b), where the position of the LCST extends over a larger temperature range. This fact is taken into account in the error estimation.

The maximum temperature difference, when going to a swelling amount of 10 % higher and lower than the swelling value at the determined LCST is used as the error of it. The approach is shown in figure 3.4 for the samples used in figure 3.3.

In figure 3.4 (a), the error of the sample with a sharp phase transition is small (the x-axis even has to be stretched, to make the error visible) compared to the sample with a broader phase transition shown in 3.4 (b). This corresponds well with the assumption, that a sharper phase transition results in a smaller error of its LCST.

### 3. Experimental Setup

---

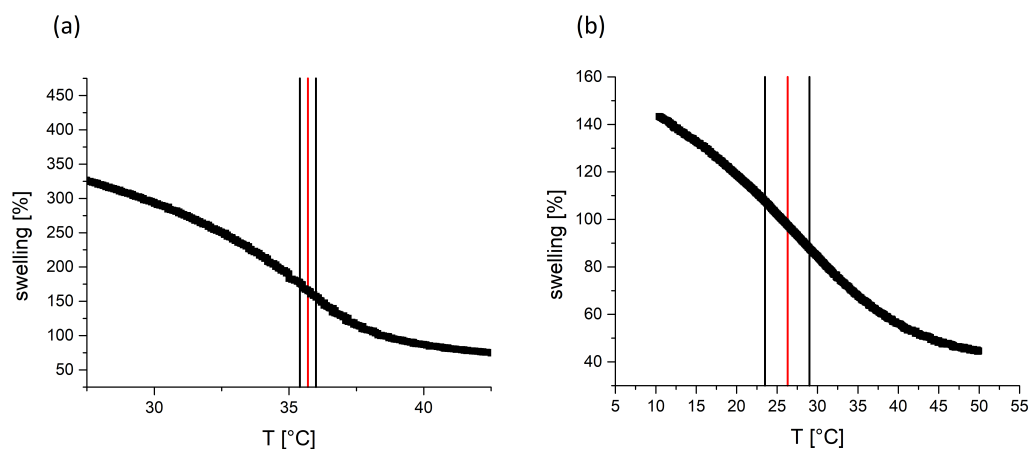


Figure 3.4.: Error estimation for (a) sharp phase transition, (b) broad phase transition

Further characterisation on the crosslinker fraction, present in the fabricated thin films, via Fourier-transform infrared spectroscopy (FTIR) is not possible, because the absorption spectra of NVCL and DEGDVE overlap. Due to the fact, that DEGDVE does not homopolymerize, no statement on the material's composition can be made out of such an experiment.

## 4. Experiments

All thin films are fabricated under the same conditions, which are given in the following list (exceptions will be described individually):

- T of NVCL-jar = 85 °C
- T of DEGDVE-jar = 70 °C
- T of substrate cooling = 35 °C
- T of filament = 200 °C
- Working pressure = 350 mTorr
- Needle valve opening of NVCL-line = at maximum
- Needle valve opening of DEGDVE-line = between 2 and 3
- Needle valve opening of TBPO-line = at 0,13 (=1 sccm)

The desired thickness of each layer is approximately 50 nm.

### 4.1. Single-Layers

On the road to thermoresponsive double-layers it is crucial to first take a look at single-layers and how their properties can be altered, to achieve good components for a film, responsive in several temperature regimes. As mentioned before, there are different approaches to change a thin film's LCST position.

### 4.1.1. Tune LCST by change of crosslinker fraction

Since a NVCL homopolymer is dissolving from a substrate, if immersed in water, co-polymerization with a crosslinking agent is necessary. As reported by Muralter et al. [13], who also used DEGDVE as a crosslinker, a nominal crosslinking fraction of 10 % has to be obtained, for producing a film, which is stable in water. A crosslinking fraction with this value will also lead to the highest degree of swelling, as well as the highest LCST, if no other techniques to change the film structure are performed.

Due to the fact, that measuring the DEGDVE fraction is difficult because this molecule does not homopolymerize and does not show a clear signature in the FTIR spectrum, the aim of the first experiment is to investigate, if the amount of swelling can be connected to the crosslinker fraction. The amount of swelling is calculate via the following equation:

$$swelling [\%] = \frac{d_{sw} - d_{dry}}{d_{dry}} * 100 \quad (4.1)$$

where  $d_{sw}$  is the film thickness immersed in water at 10 °C and  $d_{dry}$  is film thickness in dry conditions after rinsing.

To also verify the workflow of changing the needle valve position of the crosslinker-line, to alter the crosslinker-fraction in the thermoresponsive thin film, first the amount of swelling of thin films, fabricated with 3 different openings of the crosslinker needle valve are examined.

The samples are fabricated under the conditions mentioned above, with a DEGDVE needle valve opening of:

- 2 (low crosslinker fraction)
- 2,1 (medium crosslinker fraction)
- 3 (high crosslinker fraction)

## 4. Experiments

---

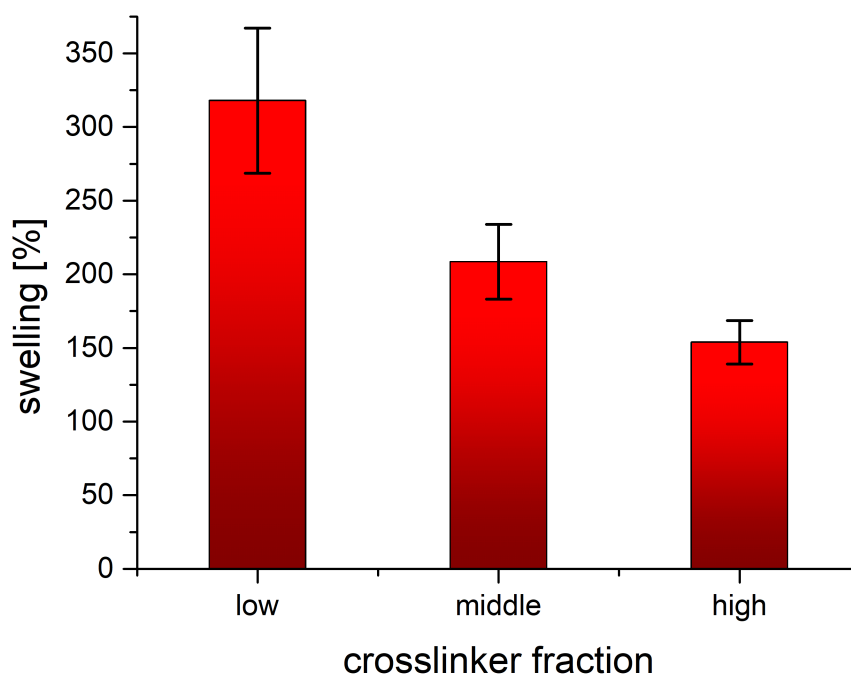


Figure 4.1.: Degree of swelling as a function of DEGDVE needle valve opening

The outcome of this experiment is illustrated in fig. 4.1

Fig. 4.1 confirms, that the workflow leads to higher fractions of crosslinker present in the fabricated thin film, if the needle valve is opened more and vice versa. With this finding, also the crosslinker fraction can be connected to the swelling behaviour, because the trend in fig. 4.1 compares well, with results given in literature.

The LCST positions, as well as the corresponding swelling curves of the films are shown in fig. 4.2

In fig. 4.2, the correlation between degree of swelling and LCST posi-

## 4. Experiments

---

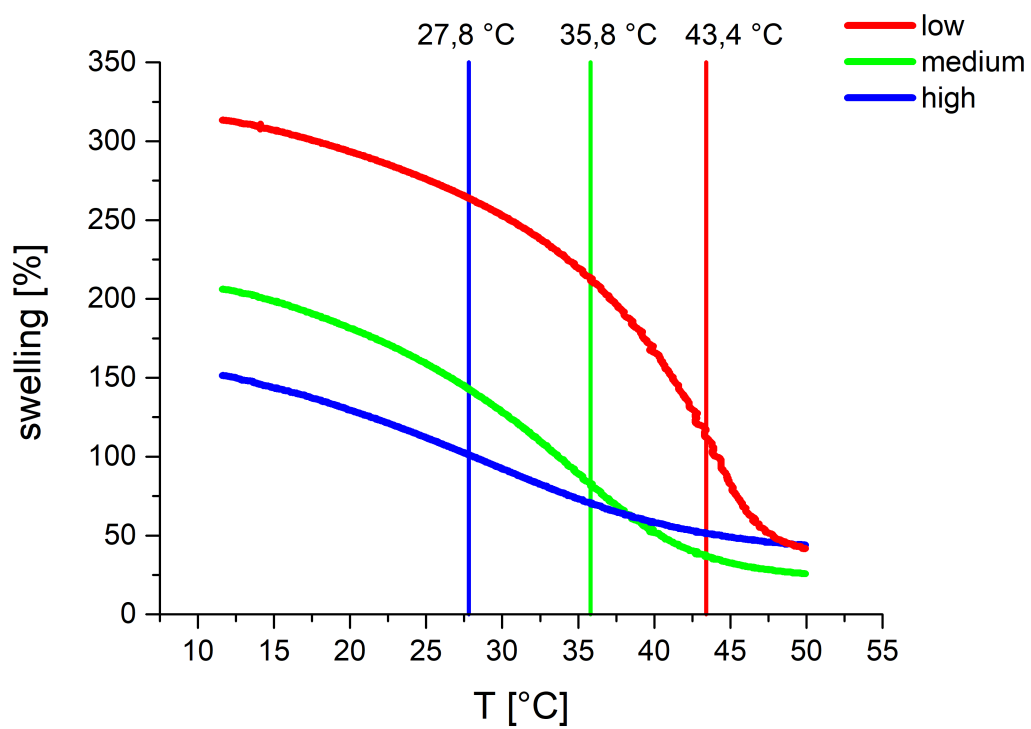


Figure 4.2.: Swelling curve and LCST position of 3 differently crosslinked films

## 4. Experiments

---

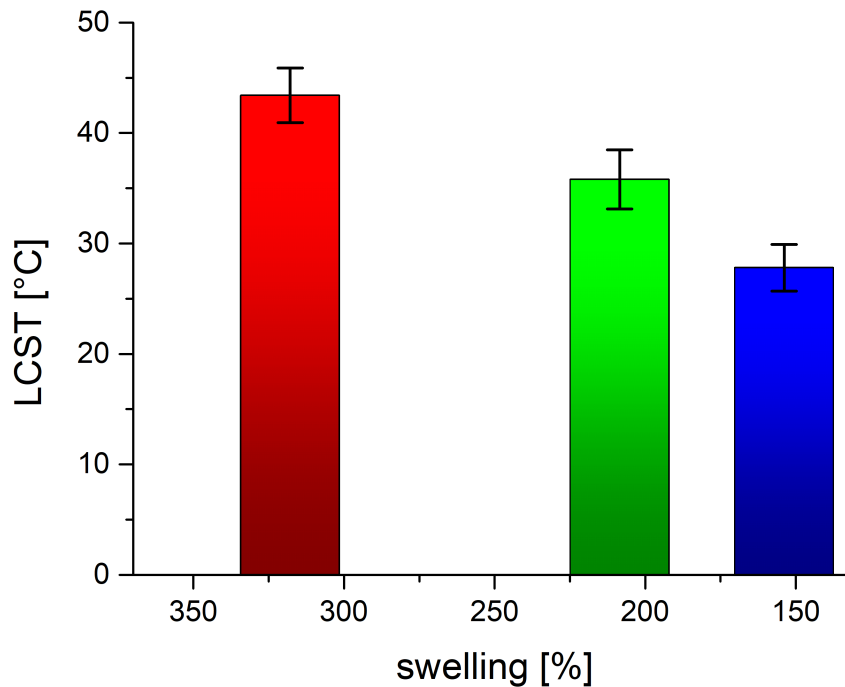


Figure 4.3.: LCST as a function of the crosslinker fraction represented by the swelling degree

tion, stemming from the modified mesh size and the altered hydrophobic/hydrophilic nature of the polymer structure, is visible. Another outcome of the experiment is that all films maintain a certain amount of swelling (30-50 %) in the collapsed state.

With this information, it is possible to plot the LCST position as a function of the crosslinker fraction represented by the swelling degree. This graph is presented in fig. 4.3

By comparing the values in fig. 4.3, with the results from Muralter et al. [13], the samples with the highest swelling behaviour and a LCST of  $43,4 \pm 0,6$

°C correspond to a crosslinker fraction of 10 %, the samples with a swelling amount of 208 % and a LCST of  $35,8 \pm 1,3$  °C correspond to a crosslinker fraction of 20 % and the samples with the lowest swelling amount and a LCST of  $27,8 \pm 2,6$  °C correspond to a crosslinker fraction of 40 %.

For the realisation of a thermoresponsive multi-layer, it is necessary to have single-layers with sharp transitions at their LCST in different temperature-regimes, as well as similar swelling behaviour. With varying the crosslinker fraction it is possible to tune the LCST, but the downside is that the higher the crosslinker fraction gets, the less thin films swell and the broader the phase transition gets. Therefore another method for changing the polymer structure has to be considered.

### **4.1.2. Tune LCST by changing the filament temperature & introducing nitrogen flow**

As mentioned in chapter 2.2.1, changing the molecular weight of the polymeric structure is leading to a change of the LCST position, without changing their ability to take up water. This is achieved on the one side, by changing the filament temperature and on the other side, by introducing nitrogen flow in the iCVD synthesis.

If the filament temperature is decreased, fewer initiator molecules getting thermally decomposed, hence less termination processes are happening, and therefore, the molecular chains can grow longer. This causes an even more open polymer mesh, which can be crosslinked to a higher quantity, resulting in a polymeric structure, with similar mesh size, but with an increased amount of hydrophobic crosslinker incorporated. Also the water repelling mechanism is enhanced with higher molecular chain length. With those two effects, thermoresponsive thin films in the temperature regime

## 4. Experiments

---

below 20 °C, but still with a suitable amount of swelling and a sharp phase transition, can be realised.

Nevertheless, without the introduction of nitrogen flow during the deposition, it has been shown by Muralter et al. [13], that lowering the filament temperature is not changing the molecular weight. An explanation for this can be, that the deposition conditions without nitrogen lead to a mass transfer-limited process, in which the filament temperature has no impact on the deposition. Through the addition of nitrogen, the working conditions seem to be in the kinetic transfer regime, where a lower filament temperature results in changes in the polymeric structure [30].

Again, 3 samples with different crosslinker fraction are fabricated under the conditions mentioned before, but with a filament temperature of 175 °C and a nitrogen flow of 1 sccm. The film with the lowest crosslinker fraction dissolved while rinsing, which can be described by the fact, that a more open mesh needs a higher amount of crosslinker incorporated, to form a stable material in water. The samples with medium and high crosslinker fraction are compared with the lowest LCST sample of section 4.1.1, the result is shown in fig. 4.4.

Fig. 4.4 indicates, that using a lower filament temperature and nitrogen flow during the polymerization process, indeed leads to lower LCSTs. Even the medium crosslinked sample of this series, exhibits a lower LCST ( $23,8 \pm 3$  °C), compared to the high crosslinked sample from section 4.1.1. The LCST of the high crosslinked sample is at  $18,4 \pm 3,5$  °C. Although the LCST position can be further decreased in this experiment, the amount of swelling decreases and the phase transition gets broader, in the same way, as for the films fabricated without nitrogen flow and a filament temperature of 200 °C. This leads to the assumption, that on the one hand the repelling mechanism in the polymeric structure is enhanced by longer molecular chains, but on

## 4. Experiments

---

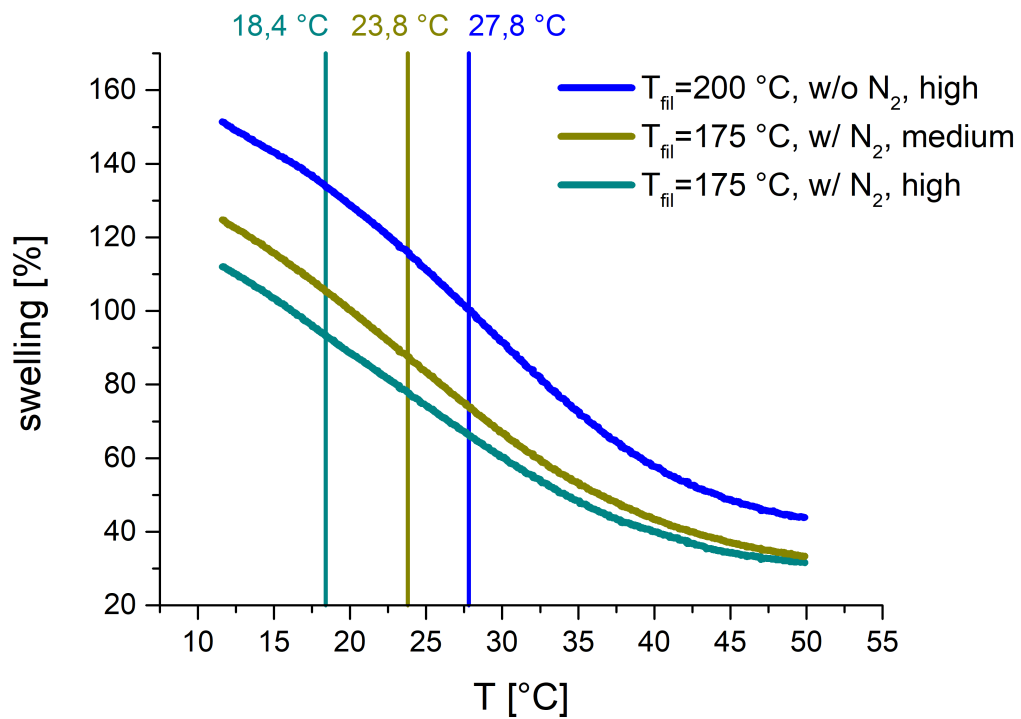


Figure 4.4.: Swelling curve of 2 differently crosslinked samples, fabricated at a filament temperature of 175 °C, compared with the highest crosslinked sample fabricated at a filament temperature of 200 °C.

the other hand the mesh is not able to take up more water molecules in the swollen state.

### 4.2. Double-Layers

Three double-layers, composed out of different single-layers are produced.

#### 4.2.1. First Double-Layer

The bottom-layer is taken from an experiment, where the influence of changing the filament temperature, without the use of nitrogen, is investigated. The result is corresponding to the experiments performed by Muralter et al. [13], which states, that there is no change of the LCST position, because of a mass transfer-limited process. Despite this finding, the synthesized thin film has a sharp phase transition at a temperature of  $37,4 \pm 0,3$  °C. The crosslinker fraction is 20 % (referring to the results of 4.1.1) and the filament temperature is at 175 °C, all other deposition settings are the same, as given in section 4. The top-layer is fabricated with the same conditions as the bottom-layer, but again with  $T_{fil} = 200$  °C, and has its LCST at  $30 \pm 4,6$  °C. The workflow of refilling the NVCL-jar after every deposition and the DEGDVE-jar after every second deposition has not been implemented at this point. This results in a poor degree of swelling of the top layer, since it is the 5th deposition, done with the same monomers (the jars are refilled prior to the bottom-layer deposition unintentionally). The resulting double-layer is shown in fig. 4.5.

The swelling curve of both single-layers and the resulting double-layer are given in fig. 4.6

## 4. Experiments

---

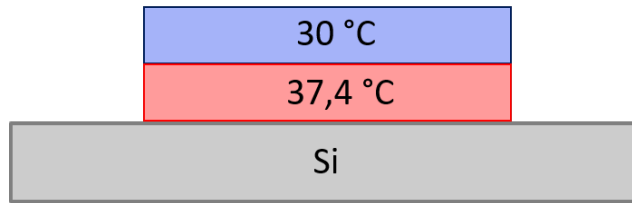


Figure 4.5.: Schematic of the 1st double-layer

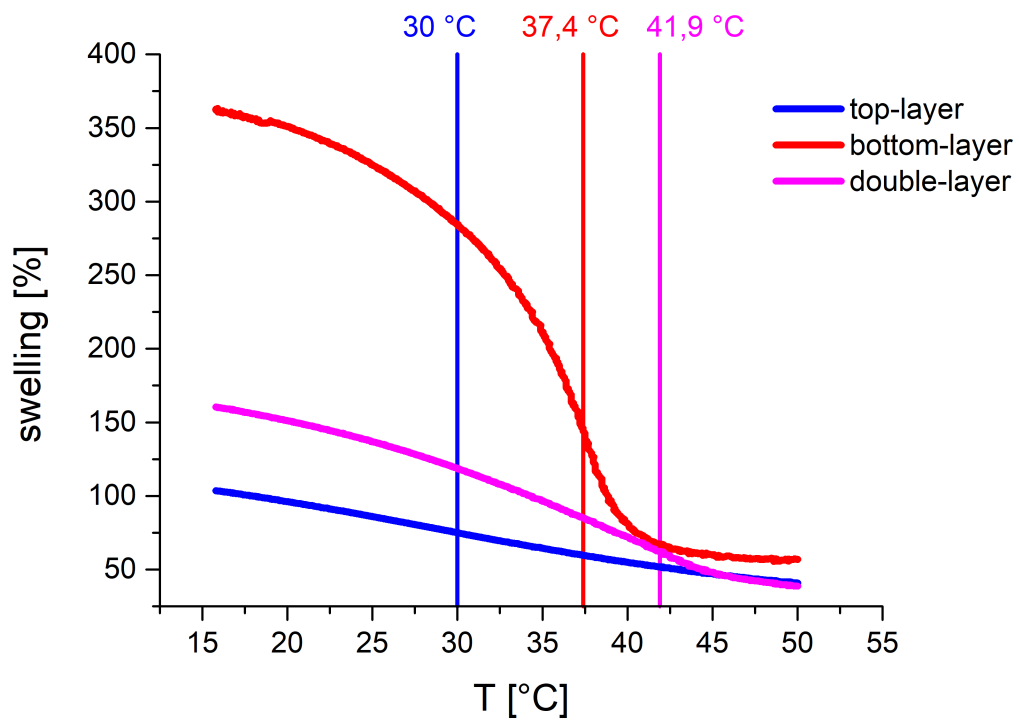


Figure 4.6.: Swelling curve of 1st double-layer and both single-layers

## 4. Experiments

---

It is visible, that the swelling curve of the double-layer is not showing two separate phase transitions. The reason for this on the one hand could be, that the phase transition of the top-layer extends over a too big temperature range, where no clear point of inflection can be seen. On the other hand the LCST positions of top- and bottom-layer are also very close, therefore the phase transitions of both layers overlap.

Furthermore, the degree of swelling is averaged between the separate swelling values of the single-layers. In addition, the LCST position of the double-layer is moved to an even higher value, namely  $41,9 \pm 1,9$  °C. This can be attributed to the fact, that the swelling mechanisms of both single-layers are not independent of each other. Apparently, while heating up the double-layer, first the top-layer collapses, which makes it harder for the bottom layer to repel the water afterwards and therefore delays the water desorption and shifts the LCST to a higher value.

To get further information about the behavior of the double-layer, its swelling curve is plotted with a theoretical, independent double-layer, constructed out of both single-layers. This graph is given in fig. 4.7

Again, two separate phase transitions can not be observed, even if the swelling mechanisms in both layers are independent, which could be explained by the fact that either the top-layer phase transition is too broad or that their LCSTs are too close. The LCST position of the theoretical constructed double-layer is exactly at the same value, as it is for the bottom-layer, suggesting that the higher swelling component is dictating the swelling behavior of the interaction-free double-layer. Another indicator that the single-layers influence each other is, the difference in the swelling degree, as well as the broadened phase transition.

The information gained from these results is, that for a thin film, which has two separate LCSTs, both components' degree of swelling should be similar, their phase transitions need to be sharp and a bigger difference of

## 4. Experiments

---

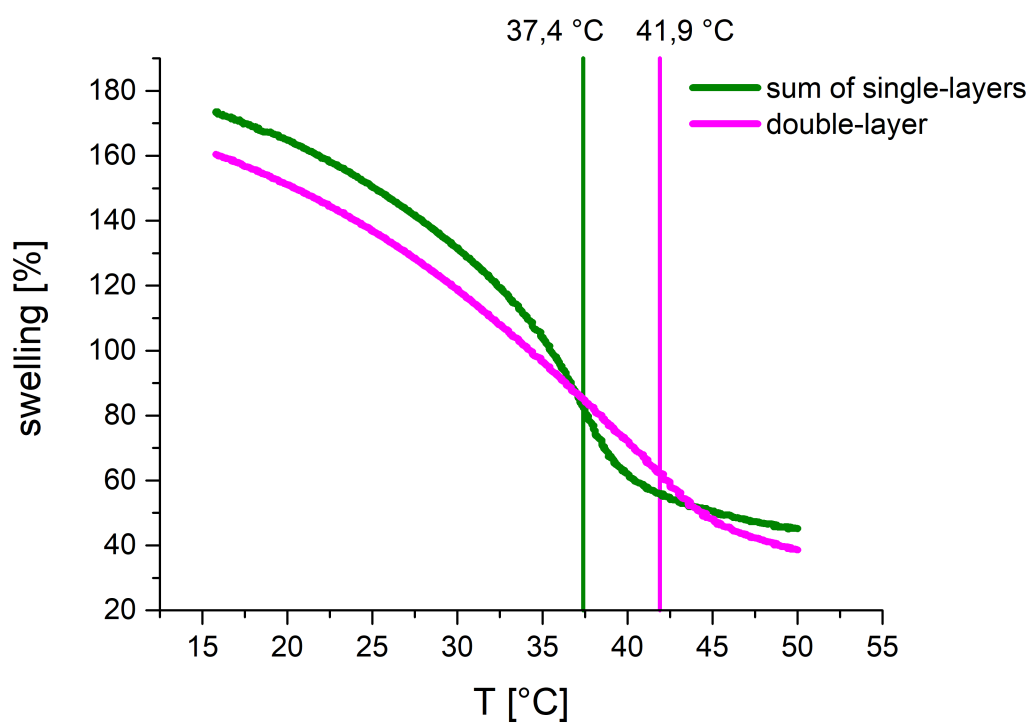


Figure 4.7.: Swelling curve of 1st double-layer and theoretical, independent double-layer

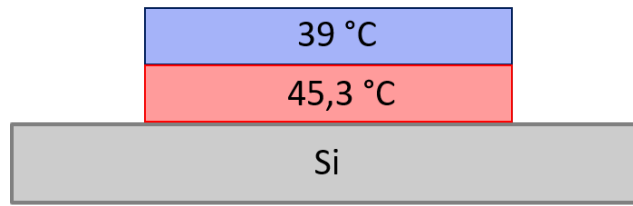


Figure 4.8.: Schematic of the 2nd double-layer

their LCST position is needed. Furthermore, the arrangement of top- and bottom-layer can also influence the double-layer's properties.

### 4.2.2. Second Double-Layer

In the second attempt, bottom- and top-layer show a comparable swelling behavior and a sharp phase transition. Both films are fabricated under the conditions give in section 4. The crosslinker fraction of the bottom-layer is at 10 % (referring to the results of 4.1.1), with a LCST at  $45,3 \pm 0,6$  °C and the crosslinker fraction of the top-layer is at 20 % and has its LCST at  $39 \pm 0,7$  °C. The structure is illustrated in fig. 4.8.

The swelling curves of the double-layer and both single-layers are given in fig. 4.9.

The first thing to mention, is that the slope of the top-layer's swelling curve has a jump at 45 °C. This has been observed over all three heating cycles, although the amount of jumps decreased over the measurements. Since a jump of this size, as well as the increase in thickness afterwards can not be explained by swelling-/deswelling-mechanisms, slight delamination could cause this conduct. The jump can also be seen in the swelling curve of the double-layer, but in an attenuated manner, where also no further increase in thickness can be seen after it, indicating stronger bonds between the

## 4. Experiments

---

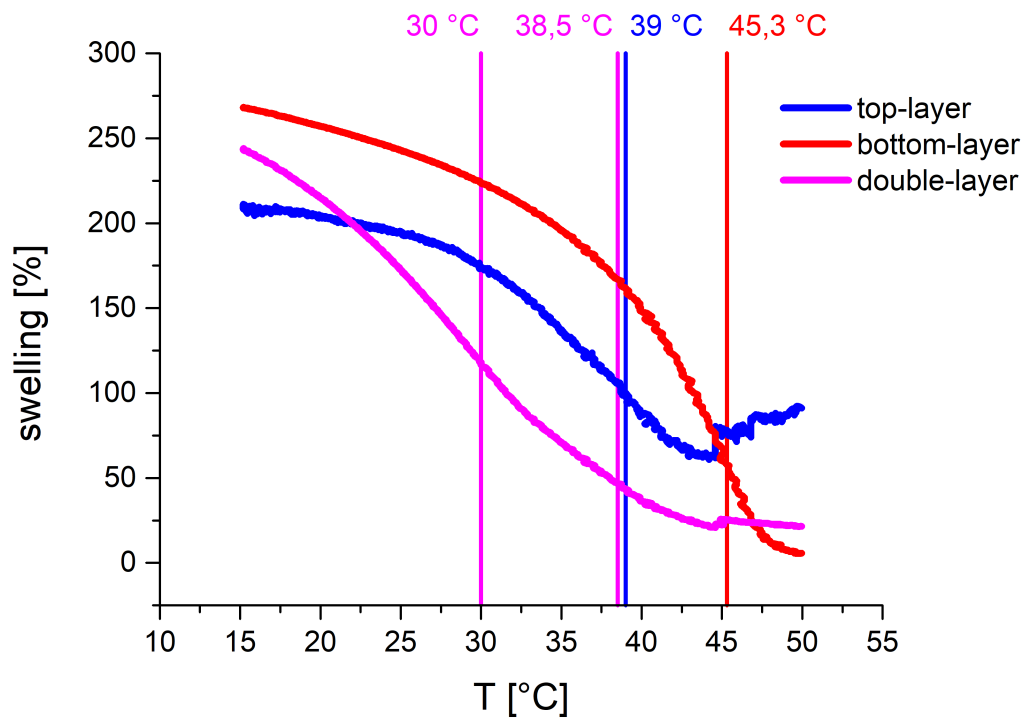


Figure 4.9.: Swelling curve of 2nd double-layer and both single-layers

## 4. Experiments

---

single-layers, than between single-layer and substrate. Fortunately in both cases, the affected films are already in the collapsed state at the position of the jump and their LCSTs can be determined without any problems.

Besides that, the swelling curve of the double-layer shows an unexpected slope. Not only, that two phase transitions are found, but also that the location of them is in a complete different temperature regime, compared to the bottom- and top-layer. Whereas the LCST of the first double-layer is shifted towards higher temperature, in this case it is shifted towards lower temperatures. The first transition is as sharp as those of the single-layers, but also is at  $30 \pm 0,9$  °C, which fits neither of them. The second LCST at  $38,5 \pm 1,5$  °C closely matches with that from the top-layer, although it is broader.

Again, the double-layer is compared with a theoretical, independent double-layer, constructed out of both single-layers (4.10).

Fig. 4.10 again suggests, that both films influence each other heavily. The deswelling-process of the double-layer starts at least 10 °C earlier than the interaction-free double-layer. Also the jump of the top-layer has to be considered, which causes the position of the theoretical LCST to be at a lower value, since the negative gradient would not decrease as much at 45 °C.

The fact, that the top-layer is collapsing prior to the bottom-layer and therefore makes water diffusion harder, which caused a shift of the LCST towards higher temperatures for the first double-layer, can not be observed within this double-layer. Despite all the unusual circumstances and the phase transition at  $38,5 \pm 1,5$  °C not being as sharp as the one at  $30 \pm 0,9$  °C, the second fabricated double-layer exhibits two LCSTs, separated by 8,5 °C.

## 4. Experiments

---

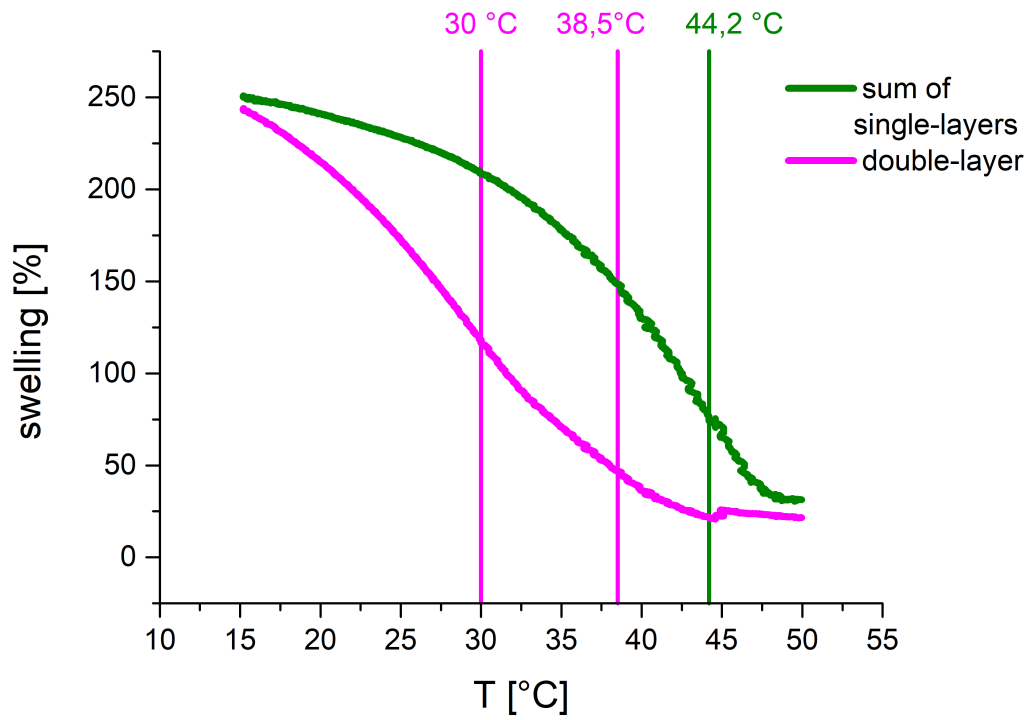


Figure 4.10.: Swelling curve of 2nd double-layer and theoretical, independent double-layer

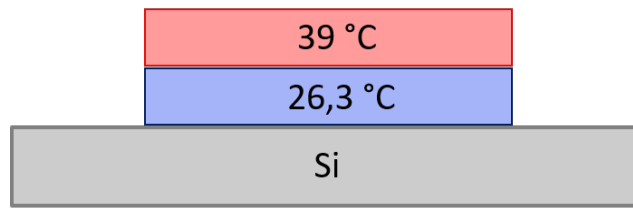


Figure 4.11.: Schematic of the 3rd double-layer

### 4.2.3. Third Double-Layer

In this section, the position of higher and lower single-layer LCST in the composed double-layer is switched. The bottom-layer is taken from an experiment, where nitrogen flow of 2 sccm is introduced in the deposition, while keeping the filament temperature at 200 °C and all other deposition settings, as described in sec. 4. With a crosslinker fraction of 20 % (4.1.1) incorporated in the thin film, a sharp phase transition at  $26,3 \pm 0,2$  °C is realized. This behavior can be explained by the fact, that slower growth kinetics, resulting from a lower  $\frac{p_M}{p_{sat}}$  value, already leads to a more open mesh size and therefore the amount of swelling of the thermoresponsive hydrogel structure increases. Attention should be paid to the part of the bottom-layer's swelling curve in the collapsed state (see 4.12). It is slightly below zero, indicating a state, where the crosslinker fraction is a bit too low, and therefore the film continuously loses thickness. By depositing another layer on top of it, further dissolution should be prevented. Also, the heating device of the Heated Liquid Cell broke during the measurement of the bottom-layer, which explains the cut-off at 38 °C. This has no impact on the LCST determination, since the bottom-layer reaches the collapsed state around 35 °C.

The top-layer is the same as for the second double-layer. The structure of the third double-layer is shown in fig.4.11.

## 4. Experiments

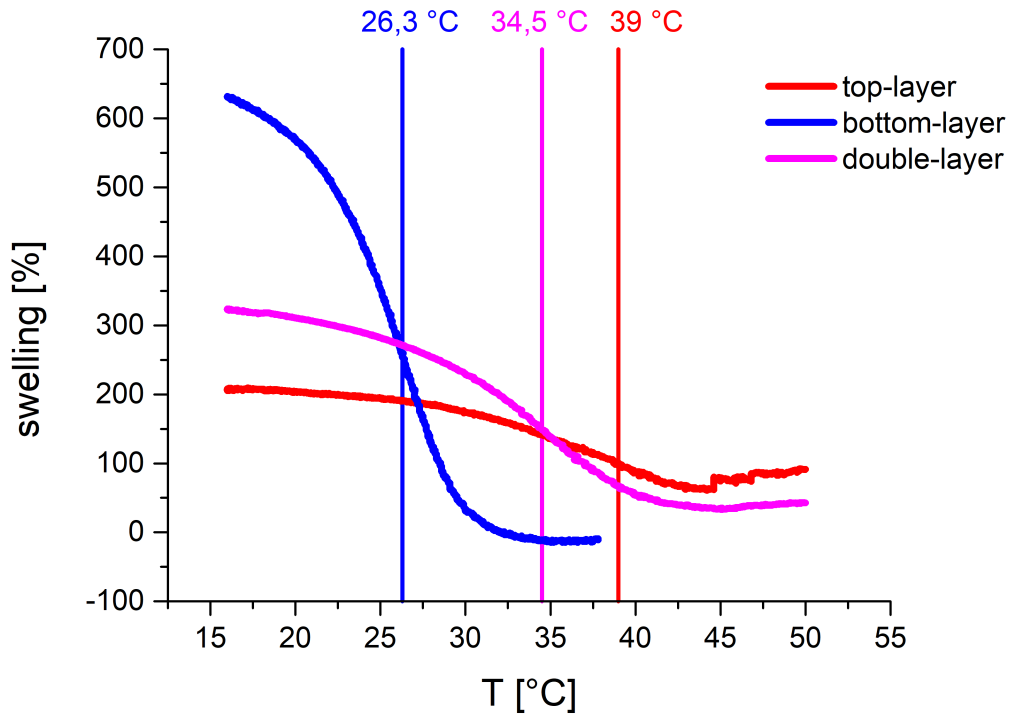


Figure 4.12.: Swelling curve of 3rd double-layer and both single-layers

In fig. 4.12 the swelling curves of both single-layers and the double-layer is presented.

Although, the positions of the single-layer's LCST are separated by around 13 °C, two discrete phase transitions can not be seen. In this case the double-layer's LCST is between the values of the single-layers, at  $34,5 \pm 0,6$  °C. This has to be an effect, stemming from interactions between top-and bottom-layer, since for this thin film the phase transitions do not overlap. As well, the instance, that the bottom-layer collapses at lower temperatures than the top-layer and therefore enables water diffusion through the swollen top-layer could be a reason for not seeing the LCST shift towards higher

## 4. Experiments

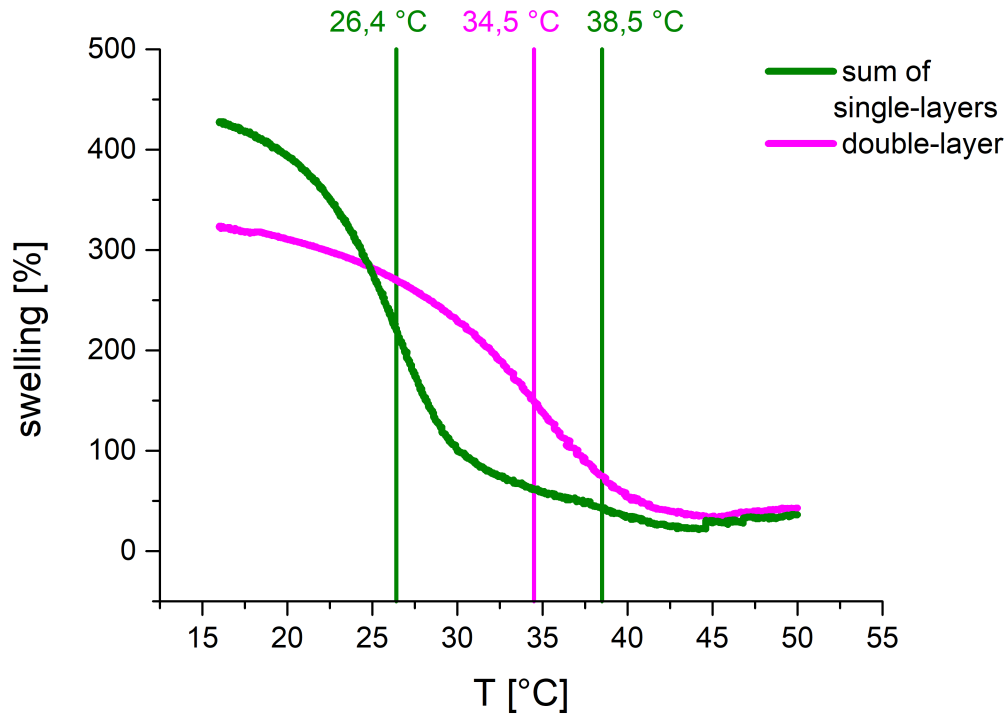


Figure 4.13.: Swelling curve of 3rd double-layer and theoretical independent double-layer

temperatures. The swelling behavior of this double-layer seems to be a combination out of both single-layers' properties, as well as the gradient of the phase transition.

The jump in the top-layer's swelling curve is not affecting the double-layers curve as much as it did in the previous section, which can be attributed to a better connection between both layers.

Again, the double-layer is compared with a theoretical, independent double-layer, constructed out of both single-layers, where the slope of the bottom-layer is assumed to be constant after reaching the collapsed state (fig. 4.13).

The swelling curves of the double-layer and the interaction-free model, again

#### 4. Experiments

---

differ from each other. The theoretical double-layer has two LCSTs, one at  $26,4 \pm 0,3$  °C and the other one at  $38,5 \pm 2$  °C. Those positions correspond to the values of the single-layers.

In comparison with fig. 4.10, the slope of both curves seem to have swapped.

## 5. Conclusion

Thermoresponsive p(NVCL-co-DEGDVE) thin films are successfully deposited via iCVD. Nevertheless, finding the right settings and working-conditions is challenging, since an abundance of parameters come into play during the polymerization process.

The low saturation pressure of NVCL and therefore its low flowrate make it impossible to predetermine the monomer ratio in the fabricated thin films. Furthermore, the absence of a method for measuring the crosslinker fraction of a deposited film, is limiting the amount of characterisation possibilities. By implementing a precise workflow and connecting the degree of swelling of a thin film to its crosslinker fraction a workaround for the challenges mentioned above, is found.

Tuning the LCST, by changing the incorporated crosslinker fraction works, as described in literature. Nevertheless, the low degree of swelling and broad phase transitions in highly crosslinker thin films, with LCSTs below 30 °C is not sufficient for the fabrication of a multi-layer, which should be responsive in different temperature regimes. To overcome this issue, the filament temperature is decreased and nitrogen flow is introduced. Lower LCSTs at lower crosslinker fractions can be obtained, since the polymeric structure is changed through this method, but the degree of swelling, as well as sharper phase transitions have not been obtained. Therefore mainly films,

## 5. Conclusion

---

where the LCST position is altered by changing the crosslinker fraction are used for the fabrication of double-layers.

Three double-layers, with different compositions, are fabricated. The first one does not show a step function, which most of all can be attributed to the bad swelling behavior and the broad phase transition of the top-layer (4.6). It also seems like the collapsed top-layer is hindering the bottom-layer to repel out the water at its LCST, which shifts the double-layer's LCST towards higher temperatures.

A step function can be obtained from the second double-layer (4.9). Although, the single-layers' LCST positions are equally apart from each other, compared with the first double-layer, the slope of the double-layers swelling curve is completely different. The fact that the first phase transition is 9 °C lower than the low LCST component and the second phase transition is approximately at the position of the low LCST component, is an unexpected result. This can only be explained by huge interactions and maybe even rearrangements between top- and bottom-layer. In addition, it has to be mentioned, that only in this double-layer, bottom- and top-layer show a similar swelling behavior.

Bottom- and top-layer of the third double-layer fulfilled almost all requirements stated, with two sharp phase transition, that do not overlap, as well as a sufficient degree of swelling (but different in their magnitude). Furthermore, the layer with the higher LCST is on top, to prevent a low water diffusion through a collapsed layer. Nevertheless, a step function can not be obtained from this double-layer and the position of its LCST is between the value of both single-layers (4.12).

All double-layers are compared with an interaction-free double-layer model, calculated out of the single-layers present in the double-layer, to gain further information about how big of an impact the layer-to-layer interaction is. The comparison of the first double-layer (4.7) shows the best match with the

## 5. Conclusion

---

theoretical thin film, which can be attributed to the badly responsive top-layer. The comparison of the other two double-layers shows big differences in the swelling curves' slope. Whereas the interaction-free model of the second double-layer (4.10) suggests only one phase transition at high temperatures, the one of the third double-layer shows two phase transitions (4.13). This is the exact opposite of the two fabricated double-layers and again, indicates strong interactions between bottom- and top-layer.

All in all, the fabrication of thermoresponsive double-layers is a really challenging task, since there are a lot of things to pay attention to. For further understanding of how the separate layers influence each other and how the double-layer's properties can be tuned, more research on this topic needs to be done.

# Appendix

# Appendix A.

## Abbreviations

<b>LCST</b>	Lower Critical Solution Temperature
<b>iCVD</b>	Initiated Chemical Vapor Deposition
<b>NVCL</b>	N-Vinylcaprolactam
<b>pNVCL</b>	poly(N-Vinylcaprolactam)
<b>DEGDVE</b>	Di(ethylene glycol) divinyl ether
<b>SE</b>	Spectroscopic Ellipsometry
<b>MSE</b>	Mean Squared Error
<b>TBPO</b>	Tert-Butyl peroxide
<b>sccm</b>	standard cubic centimeters per minute
<b>FTIR</b>	Fourier-transform infrared spectroscopy

# Bibliography

- [1] Norma A. Cortez-Lemus and Angel Licea-Claverie. "Poly(N-vinylcaprolactam), a comprehensive review on a thermoresponsive polymer becoming popular." In: *Progress in Polymer Science* 53 (2016), pp. 1–51 (cit. on pp. 1, 7).
- [2] Fabian Muralter, Francesco Greco, and Anna Maria Coclite. "Applicability of Vapor-Deposited Thermoresponsive Hydrogel Thin Films in Ultrafast Humidity Sensors/Actuators." In: *ACS Applied Polymer Materials* 2.3 (2020), pp. 1160–1168 (cit. on p. 1).
- [3] Enas M. Ahmed. "Hydrogel: Preparation, characterization, and applications: A review." In: *Journal of Advanced Research* 6.2 (2015), pp. 105–121 (cit. on p. 3).
- [4] Michael C. Koetting et al. "Stimulus-responsive hydrogels: Theory, modern advances, and applications." In: *Materials Science and Engineering: R: Reports* 93 (2015), pp. 1–49 (cit. on p. 3).
- [5] Liang-Yin Chu et al. *Smart Hydrogel Functional Materials*. Dec. 2013, pp. 1–381 (cit. on pp. 3, 4).
- [6] Stefano Palagi et al. "Structured light enables biomimetic swimming and versatile locomotion of photoresponsive soft microrobots." In: *Nature Materials* advance online publication (Feb. 2016) (cit. on p. 3).

- [7] N. Ramakrishnan et al. "Humidity sensor using NIPAAm nanogel as sensing medium in saw devices." In: *International Journal of Nanoscience* 10.01n02 (2011), pp. 259–262 (cit. on pp. 3, 6).
- [8] Stefano Fusco et al. "Shape-Switching Microrobots for Medical Applications: The Influence of Shape in Drug Delivery and Locomotion." In: *ACS Applied Materials & Interfaces* 7.12 (2015), pp. 6803–6811 (cit. on p. 3).
- [9] Paul Salzmann, Alberto Perrotta, and Anna Maria Coclite. "Different Response Kinetics to Temperature and Water Vapor of Acrylamide Polymers Obtained by Initiated Chemical Vapor Deposition." In: *ACS Applied Materials & Interfaces* 10.7 (2018), pp. 6636–6645 (cit. on p. 3).
- [10] A.K. Teotia, H. Sami, and A. Kumar. "1 - Thermo-responsive polymers: structure and design of smart materials." In: *Switchable and Responsive Surfaces and Materials for Biomedical Applications*. Ed. by Zheng Zhang. Oxford: Woodhead Publishing, 2015, pp. 3–43 (cit. on p. 4).
- [11] Ruixue Liu, Michael Fraylich, and Brian Saunders. "Liu, R., Fraylich, M. & Saunders, B. R. Thermoresponsive copolymers: from fundamental studies to applications. *Colloid Polym. Sci.* 287, 627–643." In: *Colloid and Polymer Science* 287 (June 2009), pp. 627–643 (cit. on p. 6).
- [12] Frank Meeussen et al. "Phase behavior of poly(N-vinyl caprolactam) in water." In: *Polymer* 41 (Nov. 2000), pp. 8597–8602 (cit. on pp. 6, 7).
- [13] Fabian Muralter et al. "Interlink between Tunable Material Properties and Thermoresponsiveness of Cross-Linked Poly(N-vinylcaprolactam) Thin Films Deposited by Initiated Chemical Vapor Deposition." In: *Macromolecules* 52.18 (2019), pp. 6817–6824 (cit. on pp. 6, 32, 35, 37, 39).
- [14] Bora Lee et al. "Initiated chemical vapor deposition of thermoresponsive poly(N-vinylcaprolactam) thin films for cell sheet engineering." In: 9.8 (2013), pp. 7691–7698 (cit. on p. 7).

## Bibliography

---

- [15] Fabian Muralter, Alberto Perrotta, and Anna Maria Coclite. "Thickness-Dependent Swelling Behavior of Vapor-Deposited Smart Polymer Thin Films." In: *Macromolecules* 51.23 (2018), pp. 9692–9699 (cit. on pp. 7, 28).
- [16] Eun Seok Gil and Samuel M. Hudson. "Stimuli-responsive polymers and their bioconjugates." In: *Progress in Polymer Science* 29.12 (2004), pp. 1173–1222 (cit. on p. 8).
- [17] Kenneth K. S. Lau. "Growth Mechanism, Kinetics, and Molecular Weight." In: *CVD Polymers*. John Wiley and Sons, Ltd, 2015. Chap. 2, pp. 13–44 (cit. on pp. 8, 13).
- [18] <https://www.sigmaaldrich.com/catalog/product/aldrich/139548?lang=de&region=AT>. Accessed: 2020-07-03 (cit. on p. 9).
- [19] Mahriah E. Alf, T. Alan Hatton, and Karen K. Gleason. "Novel N-isopropylacrylamide based polymer architecture for faster LCST transition kinetics." In: *Polymer* 52.20 (2011), pp. 4429–4434 (cit. on p. 9).
- [20] Tiziana Canal and Nikolaos A. Peppas. "Correlation between mesh size and equilibrium degree of swelling of polymeric networks." In: *Journal of Biomedical Materials Research* 23.10 (1989), pp. 1183–1193 (cit. on p. 11).
- [21] Kenneth K. S. Lau and Karen K. Gleason. "Initiated Chemical Vapor Deposition (iCVD) of Poly(alkyl acrylates): An Experimental Study." In: *Macromolecules* 39.10 (2006), pp. 3688–3694 (cit. on p. 11).
- [22] Kenneth K. S. Lau and Karen K. Gleason. "Initiated Chemical Vapor Deposition (iCVD) of Poly(alkyl acrylates): A Kinetic Model." In: *Macromolecules* 39.10 (2006), pp. 3695–3703 (cit. on pp. 11, 13).
- [23] H. Fujiwara. *Spectroscopic Ellipsometry: Principles and Applications*. Wiley, 2007 (cit. on p. 14).

## Bibliography

---

- [24] *Introduction to Ellipsometry*. <https://www.jawoollam.com/resources/ellipsometry-tutorial>. Accessed: 2020-04-29 (cit. on pp. 14, 17).
- [25] <https://www.jawoollam.com/resources/ellipsometry-faq#toggle-id-2>. Accessed: 2020-07-05 (cit. on p. 15).
- [26] James Hilfiker and Harland Tompkins. *Spectroscopic Ellipsometry: Practical Application to Thin Film Characterization*. Jan. 2016 (cit. on pp. 15, 16).
- [27] <https://www.jawoollam.com/resources/ellipsometry-tutorial/ellipsometry-data-analysis>. Accessed: 2020-07-05 (cit. on p. 17).
- [28] Selin Kozanoğlu, Tonguç Özdemir, and Ali Usanmaz. "Polymerization of N-Vinylcaprolactam and Characterization of Poly(N-Vinylcaprolactam)." In: *Journal of Macromolecular Science* (June 2011), pp. 467–477 (cit. on p. 22).
- [29] Abraham. Savitzky and M. J. E. Golay. "Smoothing and Differentiation of Data by Simplified Least Squares Procedures." In: *Analytical Chemistry* 36.8 (1964), pp. 1627–1639 (cit. on p. 28).
- [30] Gozde Ozaydin-Ince and Karen K. Gleason. "Transition between kinetic and mass transfer regimes in the initiated chemical vapor deposition from ethylene glycol diacrylate." In: *Journal of Vacuum Science & Technology A* 27.5 (2009), pp. 1135–1143 (cit. on p. 37).